Gas-Lifting Characteristics of Methane-Water Mixture and Its Potential Application for Self-Eruption Production of Marine Natural Gas Hydrates

Jinming Zhang [1,2,4], **Xiaosen Li** [1,2,3], **Zhaoyang Chen** [1,2,3,*] iD, **Yu Zhang** [1,2,3], **Gang Li** [1,2,3], **Kefeng Yan** [1,2,3] **and Tao Lv** [1,2,4]

1   Guangzhou Institute of Energy Conversion, Chinese Academy of Sciences, Guangzhou 510640, China; zhangjm@ms.giec.ac.cn (J.Z.); lixs@ms.giec.ac.cn (X.L.); zhangyu1@ms.giec.ac.cn (Y.Z.); ligang@ms.giec.ac.cn (G.L.); yankf@ms.giec.ac.cn (K.Y.); lvtao@ms.giec.ac.cn (T.L.)
2   Key Laboratory of Gas Hydrate, Chinese Academy of Sciences and Guangzhou Center for Gas Hydrate Research, CAS, Guangzhou 510640, China
3   Guangdong Key Laboratory of New and Renewable Energy Research and Development, Guangzhou 510640, China
4   University of the Chinese Academy of Sciences, Beijing 100083, China
*   Correspondence: chenzy@ms.giec.ac.cn; Tel.: +86-020-8705-8468

Abstract: A gas-lifting production method was firstly proposed to transport the methane-water mixture from natural gas hydrates deposits through marine vertical pipe in this work. Aiming at UBGH2-6 site, SH7 site and GMGS2-8 site, the gas-lifting performance of methane-water mixture in the vertical pipe was investigated by numerical calculation. The potential of Natural gas hydrates (NGH) self-eruption production induced by the gas-lifting process under ideal conditions was also studied based on the energy analysis. The calculation results indicate that the gas-lifting method has great advantage in avoiding the secondary hydrates formation in marine vertical pipe and reducing energy consumption. The gas-lifting process in the vertical pipe is testified to be spontaneous in UBGH2-6 site and SH7 site during the initial 4000 and 1000 days, respectively, which indicates the energy consumption for methane-water mixture transportation is saved. Sufficient heat supply for the hydrate dissociation is crucial for the NGH self-eruption production. Sensitivity analysis indicates that the water-gas ratio has more significant influences on gas-lifting performance in the vertical pipe compared to the flow rate. With the decrease of water-gas ratio, the bottomhole pressure decreases rapidly. Thus, the reduction of water production is effective to improve the gas-lifting performance.

Keywords: methane hydrates; two-phase flow; vertical pipe; gas-lifting; Natural gas hydrates (NGH) self-eruption production; bottomhole pressure

1. Introduction

Natural gas hydrates (NGH) are ice-like crystalline compounds composed of small gas molecules (<0.9 nm) and water. Generally, NGH forms in the conditions of high pressure and relatively low temperature. Guest gas molecules, such as methane, ethane, propane, carbon dioxide and hydrogen sulfide, are entrapped in the cages formed from host water molecules by hydrogen bonds. NGH has a high energy density and 1 m^3 of pure NGH contains approximate 180 Nm^3 of methane [1]. Huge amounts of NGH occur at the permafrost regions and the ocean sediments of the continental margins in nature. It is estimated that the amount of carbon in natural gas hydrates is twice the total amount of carbon in the proved fossil fuels and a consensus value of 3000 trillion cubic meters of NGH have been reached by scientists in recent years [2–4]. Accordingly, natural gas hydrate is considered

to be a potential clean energy resource in the 21st century and would be likely to meet the global expanding energy demand for the foreseeable future [5].

In 2013, Japan successfully carried out the first offshore NGH field production test using depressurization method in the Eastern Nankai Trough off the Pacific coast of Japan. This field production trial lasted for 6 days with a cumulative gas production of 120,000 Nm^3 [6]. China conducted marine NGH production test successfully for 60 days in Shenhu Area of South China Sea in 2017 using a three-phase mining technology. The cumulative gas production reached 300,000 Nm^3 [7]. However, the NGH exploitation technology is far from mature for long-term production, especially due to the high production cost and the gas hydrate bearing strata security and stability. Thus, a cost-effective and safe production technology is quite significant for NGH exploitation. Upon now, most of the researches of physical simulations and numerical simulations are focused on the gas hydrate formation and dissociation mechanisms, multiphase seepage and heat and mass transfer in the hydrate deposits. Some famous hydrate numerical simulators, such as TOUGH+HYDRATE, MH-21, STOMP-HYDRATE and CMG-STARS also concentrate on the exploitation process in sediments under seafloor [8]. However, there are few reports on two-phase flow for methane-water transportation. In NGH production process, most energy consumption is consumed in the vertical well/pipe, because the vertical well/pipe is the only path for gas collection and pumping water from sediments. Previous studies [9,10] indicate that the gas and water production rate varies very large during the long production period, which significantly affects the energy consumption for gas collection and may result in secondary gas hydrate formation during the transportation, thus the two-phase flow research in vertical pipes is necessary for further study [11].

Earlier studies point out that constant-pressure production is the most effective method for NGH production [12–14]. Methane-water fluid is driven to the production well/pipe by the pressure difference and then lifted to ocean surface through the vertical well/pipe with artificial lifting method. Low production pressure (higher than quadruple point) is commonly used in experiments and simulations of NGH production [9,15–18], because it is useful to enhance the gas production. But this approach also increases the water production simultaneously and correspondingly, the energy consumption for lifting the two-phase fluid from the bottom of the pipe to the ocean surface is significantly raised due to the large water production. According to traditional oil and gas exploitation experiences, the preferable self-eruption production could be achieved with the help of high formation pressure. However, in marine gas hydrates production, the large formation pressure usually is unavailable due to the depressurization process and low stability of hydrate strata. Zhang [19] studied the kinetic of gas lifting process with small quantity of gas methane and methane exsolution from sea water. Gas is released in the form of bubbles after a disturbance (such as a rise in bottom water temperature, landslide and et.al.) on gas hydrates and then gas bubbles in seawater may rise due to the buoyancy and carry massive surrounding seawater to form an eruption column spontaneously. This special phenomenon provides a new perspective for us to investigate the NGH production. We can take advantage of the self-eruption capability of methane-water mixture produced from NGH deposits to save energy consumption in NGH production. As sufficient gas enters the bottom of the well, the produced methane-water mixture at the bottom of the well could flow upward to ocean surface through the vertical pipe spontaneously without any pump power supply. While the gas content in the vertical pipe is insufficient, artificial lifting method is necessary. The gas-lifting system may be the most suitable way for the NGH production, since the simplicity of gas-lifting system in construction and absence of moving mechanical parts are two very important advantages that make it useful in pumping sandy and salty water [20].

In this work, a gas-lifting method was firstly proposed to transport methane-water mixture from natural gas hydrates deposits through marine vertical pipe. Aiming at the gas hydrates in Korea Ulleung Basin Gas Hydrate Second Expedition Site 6 (UBGH2-6), Shenhu area (SH7) and Guangzhou Marine Geological Survey Site 8 (GMGS2-8) in Dongsha Area of the South China Sea, the gas-lifting performance of methane-water mixture (including the original methane and injected methane) and the potential of NGH self-eruption production were investigated by numerical calculation. The effect of

water-gas ratio (R_{WG}), inner diameter (d_i) of vertical pipe and flow rate (q) on the two-phase flow were also studied. The purpose of this work is to build a simple and safe marine lifting system for accurate flow control in future NGH production and to reduce the energy consumption of NGH production by making full use of the lifting ability of the produced methane.

2. Mathematical Model

2.1. Scheme of Methane-Water Mixture Transportation by Gas Lifting

The typical gas-lifting system for marine NGH production through vertical pipe is schematically shown in Figure 1. During the depressurization production process, porous media (sand and mud etc.) and hydrates are considered to be immovable, only gas and water are movable. The pressure at the bottomhole (point A) remains constant. The pressure difference between point A and the reservoir is the driven force for NGH dissociation and fluid seepage in sediments. After methane-water mixture enters the bottom of the production well, the pressure of methane-water mixture reduces to the production pressure and it flows upward to the ocean surface along the vertical pipe driven by the buoyancy of methane bubbles.

When the produced methane in the vertical pipe is excessive to lift the two-phase fluid, the extra methane is delivered to the gas tank in store through the gas-water separator and the gas compressor. Otherwise, additional methane is injected from the offshore platform through a gas compressor. Considering the low efficiency of gas compressor at sea floor and for avoiding the pollution of the seawater, the separated water is controlled to flow to the vertical pipe. The gas injection point is at the bottom of the pipe through the annulus, which is full filled with water and gas mixture. The initial stage of gas injection as well as the corresponding effect of gas pressure on annulus fluid are not involved. In this work, only the steady state process of NGH production is considered.
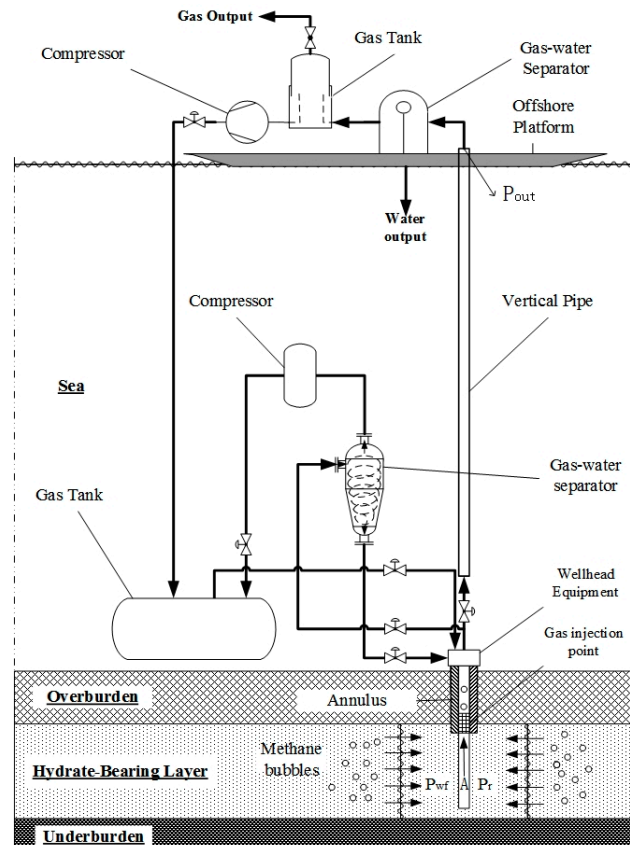

Figure 1. Typical gas-lifting system for marine NGH production.

2.2. Methane-Water Two Phase Flow Model

Compared to the vertical changes of flow parameters in the vertical pipe, the radial changes of flow parameters can be ignored. Hence, the two phase flow model in the marine vertical pipe is simplified as one dimension system. z is set as the vertical space coordinate measured directly upward. For simplicity, the production well length is incorporated into the marine vertical pipe in this study. The expression of total pressure drop is obtained based on the energy conservation [21].

$$-\frac{dP}{dz} = \rho g + \rho u \frac{du}{dz} + \frac{dP_f}{dz} \tag{1}$$

where ρ, u, g and P denote the density, flow velocity, gravitational acceleration and pressure of the methane-water mixture, respectively. The term of dP_f/dz is the pressure drop caused by the friction between the fluids and the inner wall of the pipeline, due to the lack of pipe roughness data in marine environment, a simple correlation (Blasius equation) for friction pressure drop is adopted.

$$\frac{dP_f}{dz} = C\rho Re^n u^2 / 2d_i \tag{2}$$

where $C = 64$, $n = -1$, when $Re < 3000$ and $C = 0.316$, $n = -0.25$ when $3000 < Re < 10^5$ [11]. d_i is the inner diameter of the vertical pipe. The Reynolds number of the methane-water mixture is calculated by $Re = d_i u\rho/\mu$. μ is the viscosity of methane-water mixture, which is calculated as:

$$\mu = \delta\mu_g + (1-\delta)\mu_l \tag{3}$$

2.3. State Equation of Methane-Water Mixture

In this work, the methane-water mixture is considered to be compressible. The temperature is assumed to be constant along the vertical pipe. According to Wilson's work [22], the density of methane-water mixture can be expressed as follows.

$$\frac{1}{\rho} = \frac{\delta}{\rho^g} + \frac{1-\delta}{\rho^l} \tag{4}$$

where ρ^g and ρ^l is the density of methane and water, respectively. The gas content δ is the mass fraction of the gaseous methane to the total mass of the methane-water mixture. The compressibility of seawater is ignored, hence ρ^l is constant. The composition of gas phase is assumed 100% methane. The density of gaseous methane is calculated as follows:

$$\rho_g = \frac{PM_{CH_4}}{ZRT} \tag{5}$$

where $R = 8.314$ J/mol·K, represents the ideal gas constant. M_{CH4} is molar mass of methane. T denotes the temperature of the methane-water mixture. Considering the conditions of high pressure and low temperature in the vertical pipe, S-R-K equation is adopted to determine the compressibility factor Z of methane [23].

$$Z = \frac{Pv}{RT} = \frac{v}{v-b} - \frac{a(T)}{RT(v+b)} \tag{6}$$

As the methane-water mixture flows up along the vertical pipe, the pressure decreases continuously and simultaneously, methane exsolves from methane saturated water, which results in an increase of gaseous methane content. The gas phase and water phase are assumed in equilibrium

due to the rapid dissolution and exsolution process. Based on the gas mass conservation, δ can be depicted by the following gas exsolution process:

$$\delta - \delta_0 = \frac{(1 - \delta_0)S_0}{\rho^l} - \frac{(1 - \delta)S}{\rho^l} \tag{7}$$

S is the solubility of methane in seawater, which is the function of temperature, pressure and salinity of seawater and calculated according to Duan's work [24]. S_0 is the methane solubility under bottomhole conditions. δ_0 denotes the gas mass fraction of the inlet methane-water mixture under bottomhole condition, which can be calculated from the commonly used parameter of water-gas ratio R_{WG} in previous NGH production studies.

$$\delta_0 = \frac{\rho_{ST}^g}{R_{WG} + \rho_{ST}^g} \tag{8}$$

where ρ_{ST}^g is the methane density in standard condition.

2.4. Energy Analysis of the NGH Production Process under Ideal Condition

The energy consumption of unit mass of pure gas hydrate is investigated in NGH production process, the conditions of hydrate reservoir and ocean surface are defined as the initial and final states of the methane-water system, respectively. Gas hydrate dissociation in sediments and two-phase flow in both sediments and the vertical pipe are involved in the production process. Ignored the resistance in the vertical pipe and water entrainment in the sediments, the general equation of energy consumption of unit mass of gas hydrate in NGH production is given as follows.

$$W_p + W + Q_{sur} + Q_R = \Delta E_k + \Delta E_p + Q_h \tag{9}$$

where Q_{sur} is the heat transfer from surroundings to the system, Q_R is the sensible heat release from the system during the production process. ΔE_k and ΔE_p is the change of kinetic energy and potential energy from the initial state to the final state and assuming that ΔE_k and ΔE_p are approximately zero during the seepage process in sediments due to the large resistance in porous media. Q_h is the heat used for hydrate dissociation. W is the work exchange between the system and surroundings during the production process, which includes the buoyancy work in the vertical pipe, gas expansion work in both sediments and the vertical pipe as well as the friction work during the seepage process. W_p is the input work by pump, which drives the methane-water mixture flow to the bottomhole.

For the NGH self-eruption production process under ideal conditions. As the methane-water mixture is drained from the bottomhole by its buoyancy driven, the continuous depressurization is caused in sediments and the NGH production could be achieved spontaneously. Thus W_p is removed and the energy equation could be written as:

$$W + Q_{sur} + Q_R = \Delta E_k + \Delta E_p + Q_h \tag{10}$$

The detailed calculation methods of the other items in Equation (10) are calculated by the following equations:

$$Q_h = N_h \Delta H_h \tag{11}$$

$$Q_R = C_g m_g \Delta T + C_l m_l \Delta T \tag{12}$$

$$\Delta E_k = \frac{1}{2}u^2 \tag{13}$$

$$\Delta E_p = gh \tag{14}$$

where N_h is the molar quantity of hydrate dissociation. ΔH_h = 54.1 KJ/mol, which denotes the dissociation enthalpy of methane hydrate [25]. C_g and C_l are the specific heat of gas and water,

respectively, m_g and m_l are the methane and water mass released from unit mass of hydrate, respectively. ΔT is the temperature difference between the hydrate reservoir condition and the condition in the vertical pipe. Gas expansion work and friction work during the seepage process is converted to the internal change of the system. Thus the work exchange between system and surroundings W during the vertical flow process can be calculated through a dynamics of reversible gas-driven eruption process [26]. Which is equal to the buoyancy work minus gas expansion work.

$$W = -\int \frac{1}{\rho} dP \tag{15}$$

To solve Equation (15), a simplified formula is derived according to Zhang's method in this work [26]. Combining Equations (3)–(6), the expression of state for methane-water mixture is derived:

$$\frac{\rho_0}{\rho} \approx 1 - S + S_0 \frac{ZP_0}{Z_0 P} \tag{16}$$

And correspondingly, the expression of work exchange between the system and surroundings is updated.

$$W \approx -\frac{1}{\rho_0} \int_{P_0 - \Delta P}^{P_{out}} (1 - S + S_0 \frac{ZP_0}{Z_0 P}) dP \tag{17}$$

where ρ_0 and P_0 are the density and pressure of methane-water mixture under the reservoir condition. P_{out} is the outlet pressure at ocean surface. ΔP is the pressure loss in sediments during the seepage process. Which is given according to the radial fluid flow in unit thickness sediment.

$$\Delta P = \mu \frac{q}{\rho} \frac{\ln \frac{2r_w}{d_i}}{2\pi K} \tag{18}$$

In Equation (18), the methane-water mixture is treated as homogeneous. K is the permeability of the hydrate-bearing layer, r_w is the radius of the hydrate-bearing layer, which is set to be 125 m in this work. In the NGH self-eruption production, the small amount of heat to work conversion during the hydrate dissociation is ignored, thus the heat for hydrate dissociation is considered to be supplied by Q_R and Q_{sur} and the energy consumption for lifting methane-water mixture to the ocean surface is provided by buoyancy work from bottomhole fluid.

2.5. Computational Method

Typical top-down pressure-traverse calculation with a constant outlet pressure of 0.2 MPa (higher than the pressure of the atmosphere) is adopted in this work. The exsolution process makes the top-down pressure traverse calculation difficult, because S_0 in Equation (6) is determined by the bottomhole pressure, while the bottomhole pressure is unknown before calculation. To handle this problem, an additional iterative loop is added in calculation program, a pre-estimated value of bottomhole pressure is given to carry the calculation and then the pre-estimated value is updated by the calculated bottomhole pressure. When the calculation is convergent, the exsolution process could be described accurately.

3. Results and Discussion

3.1. Model Validation

Due to the lack of NGH field production data, the calculation model was validated by comparing the pressure prediction performance of our model with other six widely used models. We calculated the pressure distribution of oil-water-gas three phase fluid (considering the oil and water to be liquid phase) flowing upward through a 3000 m vertical pipe. The results are shown in Figure 2. In this

case, gas-liquid ratio is 64.84 Nm^3/Nm^3, water cut is 20%, gas-liquid flow rate q is 5.1639 kg/s and d_i is 0.0620 m. In these models, Hagedorn and Brown's model [27] only involved the effect of slip velocity, while the others took the flow pattern transition into account. The minimal and maximal P_{wf} is proposed by Orkiszewski [28] and Aziz's [29] models, respectively, with a discrepancy of nearly 30%. The result of Ansari's model [30] is 5% different from that calculated by Beggs and Brill's model [31], while Mukherjee and Brill's [32] result is nearly identical to that of Aziz's. P_{wf} of our model shows 2% deviations from Ansari's model and less than 2% deviations from the average values. In Figure 3, the bottomhole pressure prediction performance of our model and HK's model [21,33] were calculated by using field data (Table 1) from Orkiszewski's work [28]. Most calculated data points are within ±10% error bands, which indicates a good performance of our model. Previous studies declare that the phase slippage and flow pattern transition have effects on the pressure distribution and complex corrections are involved to calculate the mixture density [34–36] but the fully developed empirical correlations are confined in a small range of application and no models has emerged as single most reliable [11,21]. In NGH production, empirical correlations for specific conditions may not be suitable, because the flow rate q and gas content δ vary much during the production period. Compared to the traditional models, a great advantage of our model is the simplicity because no complex empirical formula is needed.
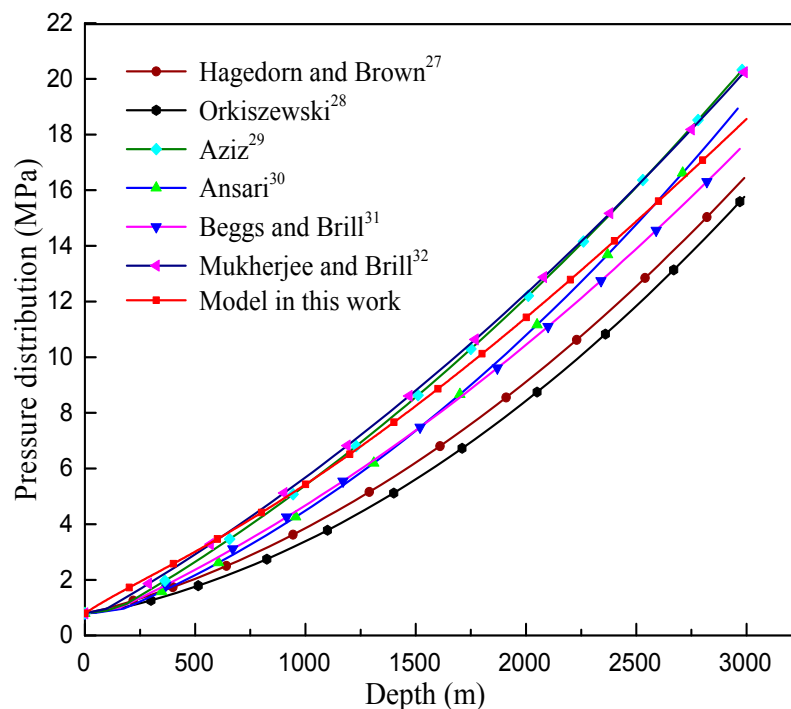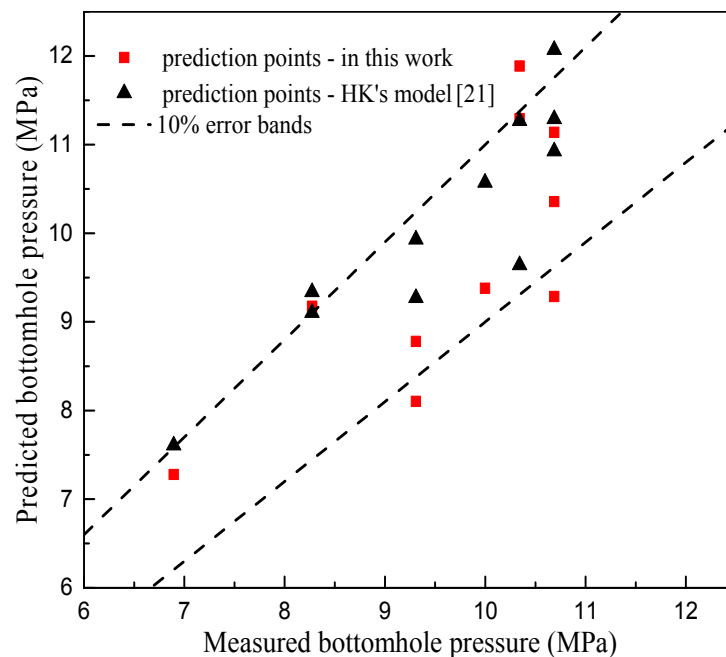

Figure 2. Pressure distributions obtained from different models.

Table 1. Range of variables used in the validation study.

Variables	Maximum	Minimum
q **(kg/s)**	**5.0000**	**1.7968**
Gas content (kg/kg)	0.1480	0.03334
Pipe Length (m)	1453	1129
P_{wf} (MPa)	10.6869	6.8948
P_{out} (MPa)	4.8263	1.0342

Figure 3. Bottomhole pressure prediction performance comparison of HK model with our proposed model.

3.2. Evaluation of Gas-Lifting Method on NGH Production

3.2.1. Advantages of Gas Lifting Method in NGH Production

Aiming at three typical NGH reservoirs in UBGH2-6 site, Shenhu SH7 site and GMGS2-8 site, we carried out gas-lifting study in vertical pipes. The basic flow parameters used in this work are listed in Table 2. The progress of pressure and temperature near the bottomhole during the depressurization production process of these three cases are schematically shown in Figure 4. The constant production pressure P_r are employed in these three cases. During the depressurization process, the pressure reduces isothermally from the reservoir pressure (point A) to point B (slightly lower than hydrate phase equilibrium pressure) at first, then gas hydrate dissociates and the temperature decreases, simultaneously, the temperature and pressure conditions of the hydrate shift toward point C along the hydrate phase equilibrium curve. At last, the pressure reduces isothermally from point C to the production pressure P_r (point D) after the hydrate near the bottomhole dissociates completely. The temperature at point D is the temperature in pipe.

Table 2. Flow properties used in the study of references cases.

Variables	UBGH2-6 [18]	GMGS2-8 [37]	Shenhu SH7 [9]
q (kg/s)	0.6465–18.6446	21.87–61.03	10.46–44.8
R_{WG} (kg H_2O/Nm^3 CH_4)	5–117	198–952	189–1571
Pipe Length (m)	2320	875	1274
Salinity (%)	3.50	3.50	3.05
Production pressure (MPa)	3.0	4.5	10.96
Inner diameter (mm)	200	200	200
Temperature in pipe (K)	280	279	286.5
Reservoir temperature (K)	289	280.5	287
Reservoir pressure (MPa)	23	9	13.83
Reservoir boundary	Impermeable	Permeable	Permeable
Permeability of HBL (mD)	500	7500	-

The bottomhole pressure (P_{wf}) is the minimum pressure needed to lift the methane-water mixture to the ocean surface through the vertical pipe. The water-gas ratio R_{WG} and flow rate q used for the P_{wf} calculation were adopted from the Tough+hydrate depressurization simulation results of other researchers [9,18,37]. As can be seen from Figure 4a,b, the calculated average P_{wf} at GMGS2-8 site and SH7 site are higher than the corresponding production pressure of 4.50 MPa and 10.96 MPa, respectively. Meanwhile, the points of P_{wf} in these two cases both are located in hydrate stable zone. This implies that the artificial lift method is needed to transport the methane-water mixture from the bottomhole to the ocean surface in both cases. If the submersible pump is employed to raise the fluid pressure from P_r to P_{wf}, the methane-water mixture would enter the hydrate stable zone inevitably and result in the secondary hydrate formation, which possibly leads to a consequent detriment of pipe blockage. However, the gas-lifting method proposed in this work can effectively avoid this hazard of secondary hydrate formation. In GMGS2-8 site and SH7 site, the additional gas injection of 10^5 Nm^3/d could reduce the average P_{wf} from 11.97 MPa and 7.98 MPa to 8.13 MPa and 3.41 MPa, respectively.

In UBGH2-6 site, the average P_{wf} is 2.40 MPa (Figure 4c), which is lower than the corresponding P_r. It means the gas-lifting process of methane-water mixture in the vertical pipe could be spontaneous in UBGH2-6 site, such spontaneous gas-lifting process is driven by the buoyancy of methane bubbles and the additional energy consumption for gas injection is avoided. Meanwhile, secondary hydrate formation would not occur in the vertical pipe.
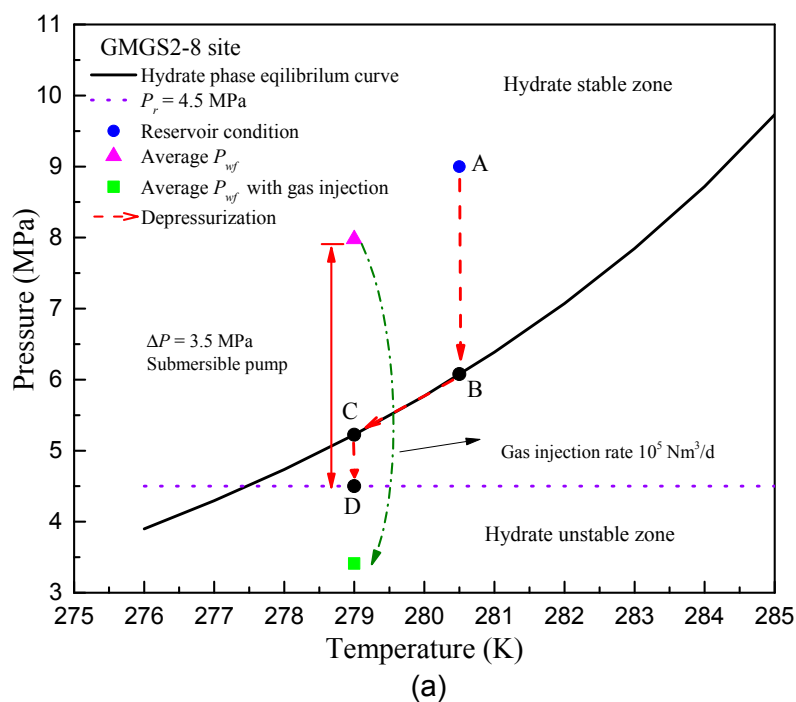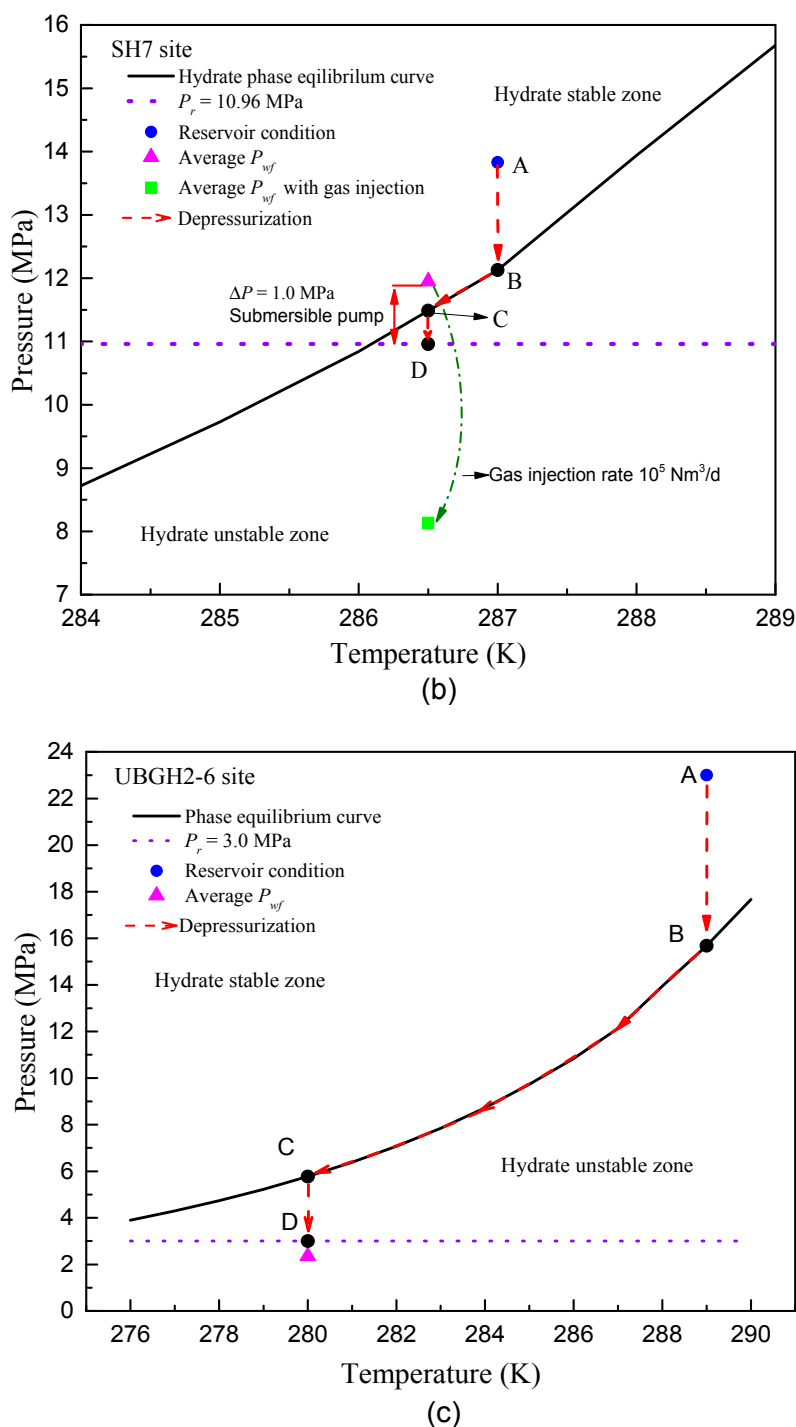

Figure 4. *Cont.*

(b)

(c)

Figure 4. Variation of temperature and pressure conditions during the NGH production at different reservoir. (**a**) GMGS2-8 site; (**b**) SH7 site; (**c**) UBGH2-6 site.

3.2.2. Gas-Lifting Performance of Methane-Water Mixture

The calculated P_{wf} over time in UBGH2-6 site is shown in Figure 5a. P_{wf} without gas injection shows a rapid decline in the initial 500 days and maintains lower than P_r for nearly 4100 days due to the relatively low R_{WG} in produced methane-water mixture. During this period, the produced methane in the vertical pipe is sufficient to lead a spontaneous gas-lifting process. After 4100 days, as the R_{WG} increases, the calculated P_{wf} starts to increase and exceeds P_r in the rest period of production. At the end of production period, P_{wf} reaches a maximum of ca. 20 MPa. The additional gas injection is needed

to maintain the production. The calculated P_{wf} decreases with the increase of gas injection rate. When the gas injection rate reaches 10^4 Nm^3/d, the P_{wf} stays lower than P_r during the whole production process. The minimum of P_{wf} decreases to less than 1 MPa because the gas injection greatly decreases R_{WG}. Under the gas injection rate of 10^4 Nm^3/d, the gas-lifting performance in the vertical pipe is improved significantly.

The calculated P_{wf} (Figure 5b) without gas injection over time in GMGS2-8 site is characterized by an initial increase and remains stable until the end of production period. The P_{wf} is higher than P_r in all the production period, which indicates that the gas injection in the vertical pipe is necessary in this case. With a gas injection rate of 10^5 Nm^3/d, the P_{wf} still stays above P_r except for the initial 4000 days. This indicates that the gas-lifting performance of methane-water mixture is poor in GMGS2-8 site. Compared to UBGH2-6 site, the P_{wf} in UBGH2-6 is much lower than that in GMGS2-8 site and gas injection has a better effect on P_{wf} reduction in UBGH2-6 site, though the production pressure P_r employed in both cases are close. In UBGH2-6 site, the overburden and underburden are considered to be impermeable, thus the R_{WG} of the methane-water mixture produced from the deposits is low. However, in GMGS2-8 site, overburden and underburden are permeable. The large amount of water flow through permeable boundaries into the hydrate deposits limits the effectiveness of depressurization and results in substantial water production, additionally, the gas loss through the overburden are large [18].

The calculated P_{wf} without gas injection in SH7 site (Figure 5c) increases rapidly in the first 1000 days and remains stable afterwards. The P_{wf} is less than P_r in the initial 1000 days, hence the gas-lifting process is spontaneous in this period. After 1000 days, the P_{wf} stays closely to P_r, which implies a relatively small amount of gas injection rate required compared to that in GMGS2-8 site. With a gas injection rate of 10^5 Nm^3/d, the P_{wf} reduces to far less than P_r. Overall, the P_{wf} curve in SH7 shows no significant difference from that in GMGS2-8 site (Figure 5b), because the reservoir properties in these two sites are similar and the two boundaries are permeable strata. However, the gas-lifting performance of methane-water mixture is poor in SH7 site but is significantly improved because the higher P_r. It is because the higher P_r leads to the small water production. Thus, higher P_r is suggested in permeable boundaries for NGH production.
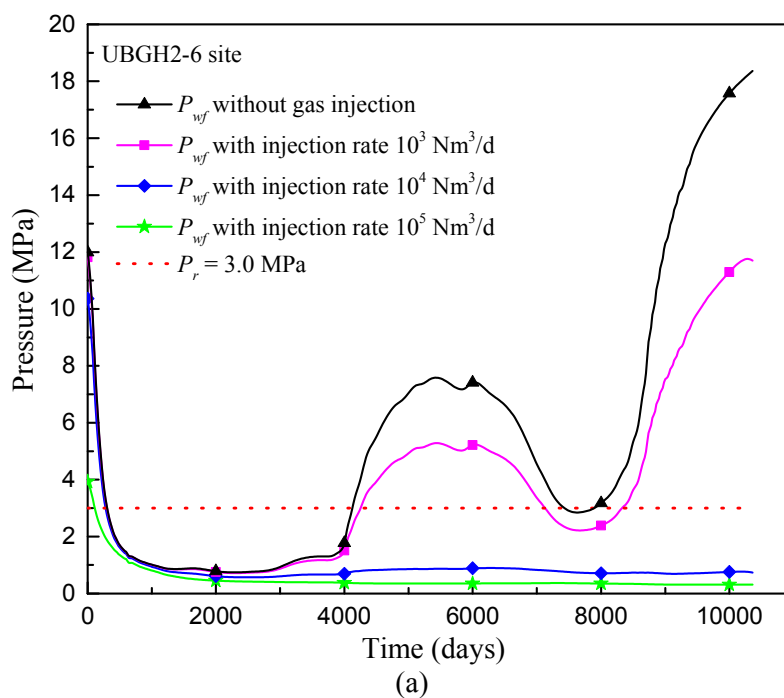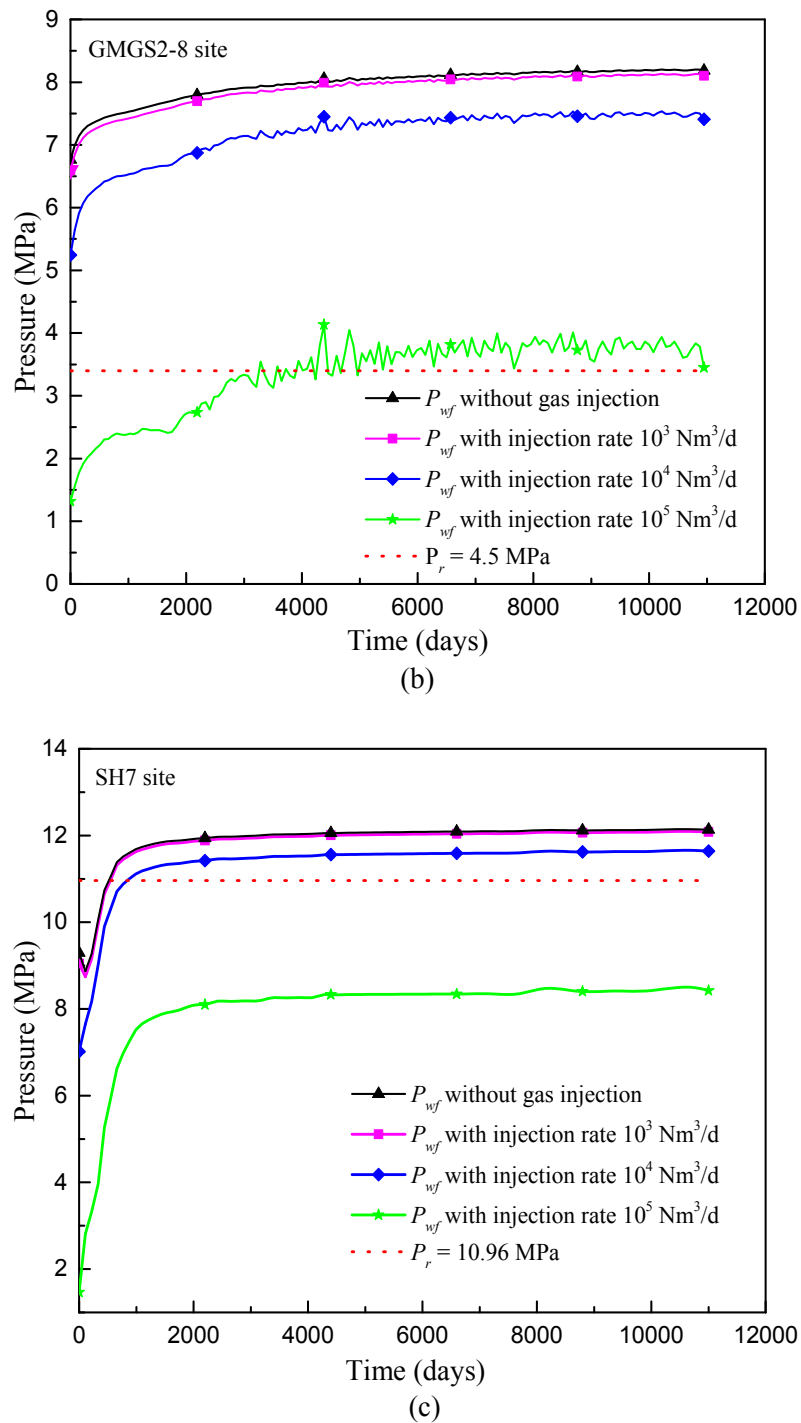

Figure 5. *Cont.*

Figure 5. Calculated bottomhole pressure with gas injection in the vertical pipe at different reservoirs. (**a**) UBGH2-6 site; (**b**) GMGS2-8 site; (**c**) SH7 site.

3.2.3. Energy Consumption of NGH Self-Eruption Production

Figure 6 shows the energy consumption of unit mass gas hydrate in NGH self-eruption production process. In UBGH2-6 site, the work exchange between the system and the surroundings is −37.4 KJ/kg, the negative sigh means the work is done to the methane-water mixture system. Considering that the energy consumption for lifting unit mass of methane-water mixture from sediments to the ocean surface (ΔE_p) is only 23.2 KJ/kg, which indicates that energy consumption for fluid transportation is totally provided by the buoyancy work done to the system from the bottomhole fluid and thus artificial

lift method is unnecessary. Under the conditions of UBGH2-6 site and GMGS-8 site, the energy consumption for fluid transportation are close, it is because that the relatively low permeability of HBL in UBGH2-6 site causes more pressure loss during the seepage process. We can conclude that in self-eruption production process, the energy input is the heat supply from surroundings to the system (Q_{sur}). As is shown in Figure 6, Q_{sur} is much larger than the energy consumption for fluid transportation, although there are slight differences in these two cases due to the sensible heat release during the hydrate dissociation. This indicates that sufficient heat supply from surroundings to gas hydrate is crucial for the self-eruption production. Such heat energy might be provided by the relatively warmer water below sediments or by electric heating. Considering a more realistic self-eruption process, the actual flow rate at the ocean surface may be significantly higher than 1 kg/s, because massive entrainment water is involved. Actually, the NGH self-eruption production is likely to be feasible, once the depressurization operation is carried out in the NGH reservoir and if low R_{WG} of methane-water mixture is produced, the self-eruption production might be realized. However, a matter of concern is that such eruptions not only provides a new way for energy saving but also presents a possibility for geo-hazard. For an uncontrollable methane eruption, the rapidly dissociated CH_4 might flow upward directly instead of entering the vertical pipe, the rapid up-flow gas-water column could lead to a serious geo-hazard, such as seawater pollution, the greenhouse effect and even a submarine landslide. A similar powerful eruption process has been observed in Lake Monoun and Lake Nyos [26,38,39]. Therefore, study on controllable self-eruption production is necessary in future NGH production.
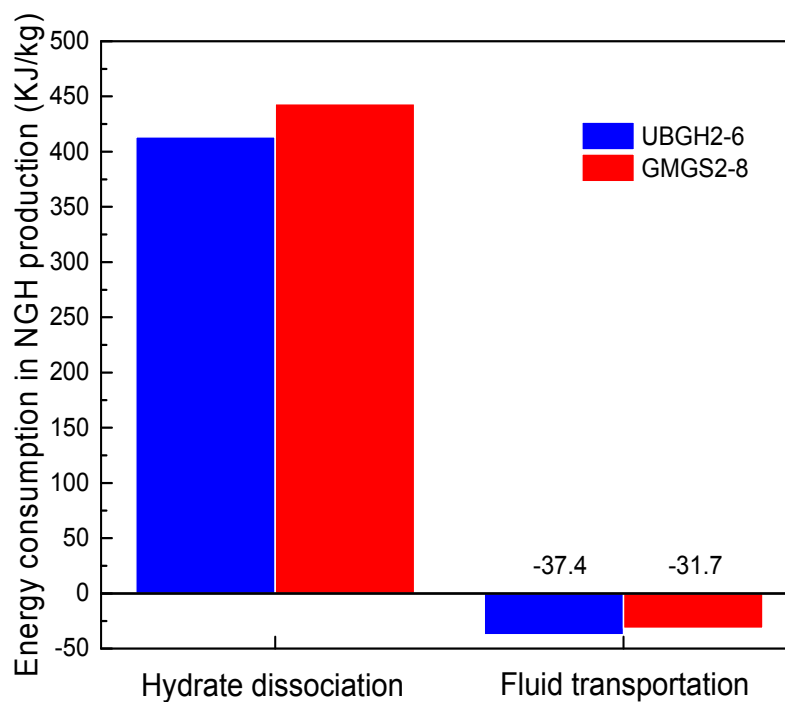

Figure 6. Energy consumption of unit mass methane hydrate in self-eruption production.

3.3. Study on Sensitivity Parameters

3.3.1. Effects of Inlet Water-Gas Ratio

As mentioned above, the inlet R_{WG} varies dramatically with production period and reservoir conditions. Gas injection rate is essentially to increase the inlet R_{WG}. The effects of inlet R_{WG} on the pressure, velocity and density distributions along the vertical pipeline are shown in Figures 7–9, respectively. The inlet R_{WG} = 5, 20, 50, 100, 200, 500 kg H_2O/Nm^3 CH_4 are employed. The

minimum inlet R_{WG} = 5 kg H_2O/Nm^3 CH_4 is selected from the simulation results of UBGH2-6 site [18]. The maximum of inlet R_{WG} = 500 kg H_2O/Nm^3 CH_4 denotes the extreme case, the produced methane is dissolved in seawater and gas phase at the bottom of the pipe is approximately considered to be absence.

The pressure gradient decreases with the decrease of pipe depth (Figure 7). In case of R_{WG} = 500 kg H_2O/Nm^3, the pressure distribution in the vertical pipe is approximately linear, which is similar to the static pressure of seawater, because only small amount of methane exists at the bottom of the pipe and besides, the effect of methane exsolution on flow is weak. With the decrease of R_{WG}, pressure distribution becomes gentler. Especially in the case of R_{WG} = 5 kg H_2O/Nm^3, the pressure distribution is almost constant. The effect of R_{WG} on the P_{wf} with different pipe length (reservoir depth) is shown in Figure 8. In each case of pipe depth, P_{wf} decreases with the decrease of R_{WG}. As R_{WG} decreases from 500 kg H_2O/Nm^3 CH_4 to 5 kg H_2O/Nm^3 CH_4, P_{wf} decreases to a low level and when R_{WG} is smaller than 100 kg H_2O/Nm^3 CH_4, the decrease of P_{wf} is rapidly. This indicates that the lower R_{WG} has more significant influence on P_{wf}. P_{wf} decreases to less than 2 MPa at R_{WG} = 5 kg H_2O/Nm^3 CH_4 in each pipe depth. Such low P_{wf} implies that the gas-lifting performance is significantly improved at low R_{WG}, hence the reduction of water production is effective to improve the gas-lifting performance of methane-water mixture. P_{wf} calculated based on a shorter pipe is lower compared to the longer pipe, it is because the pressure drop caused by gravity is small—this indicates that the gas accumulations in shallower sediments is easier to exploit.

In the case of R_{WG} = 500 kg H_2O/Nm^3 CH_4, the density of water-gas mixture decreases from 1035 kg/m^3 to less than 300 kg/m^3 at the ocean surface and the flow velocity increases slightly from 0.3 m/s to 1.20 m/s. Under the condition of R_{WG} = 5 kg H_2O/Nm^3 CH_4, the flow velocity at the ocean surface exceeds 25 m/s, the density of mixture remains in a low level with approximate linear pattern and decreases to less than 50 kg/m^3 at the ocean surface. Notice that in Figures 9 and 10, there are inflection points on the density distributions and the velocity distributions, with the decrease of R_{WG}, the inflection point moves to a deeper position. Gas phase exists in the form of bubbles in pipes, the gas bubbles flow up through vertical pipe due to the buoyancy of low density fluid, the volume of gas bubbles expands with the reduction of pressure, hence the density of bubbly water decreases and leads to a more rapid rising, this is a strong positive feedback process [19]. With the decrease of R_{WG}, gas content increases in pipes and this process starts earlier.
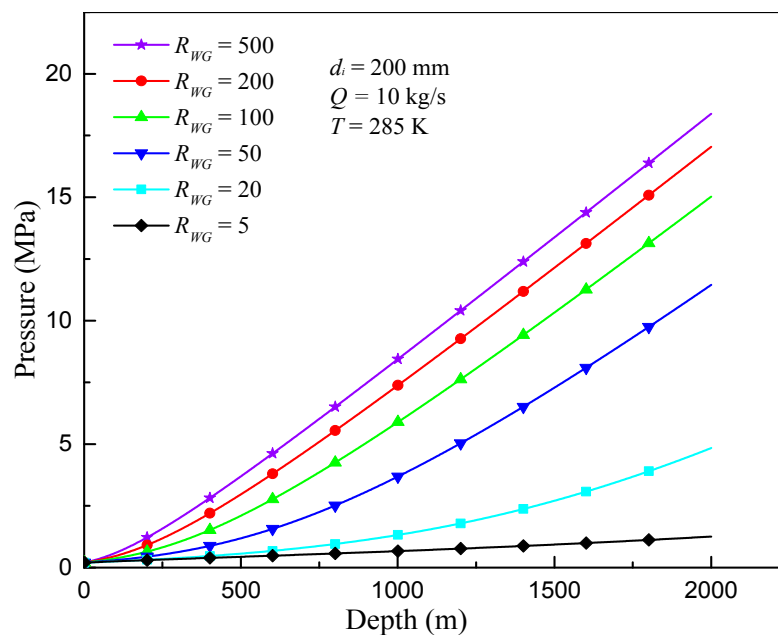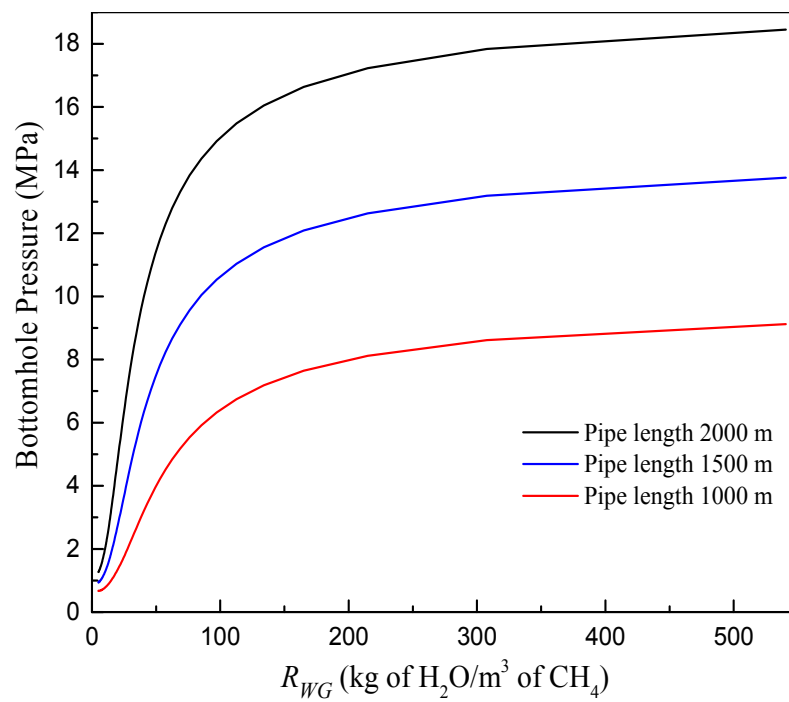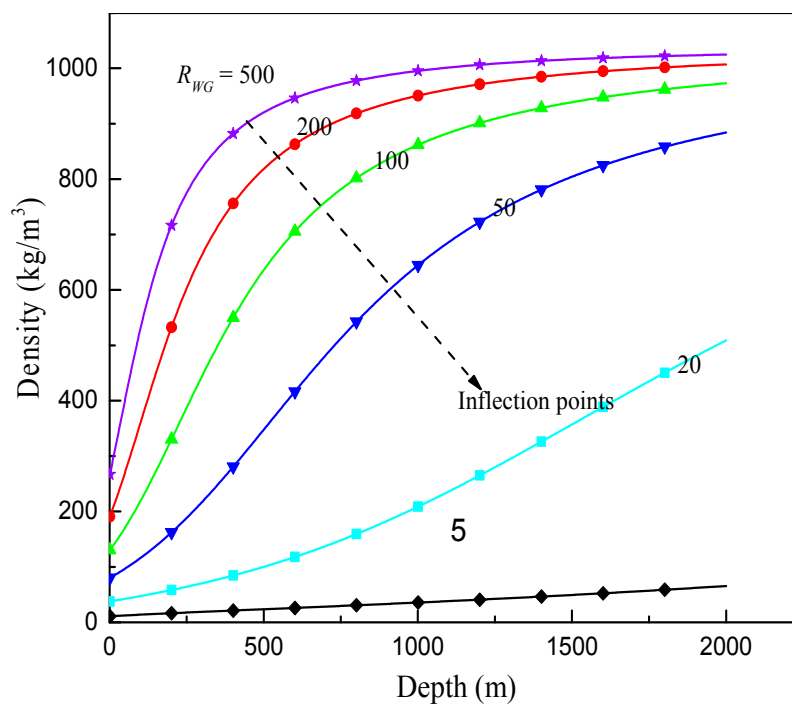

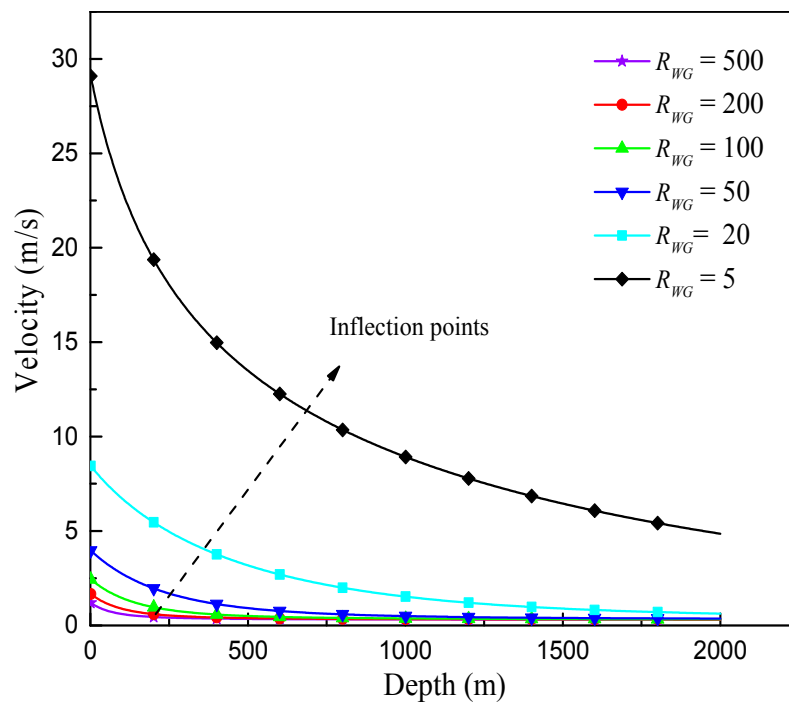**Figure 7.** Pressure distributions along the vertical pipe under different R_{WG} (kg H_2O/Nm^3 CH_4).

Figure 8. Effect of water-gas ratio (R_{WG}) on the bottomhole pressure with different pipe length.

Figure 9. Density distributions along the vertical pipe under different R_{WG} (kg H_2O/Nm^3 CH_4).

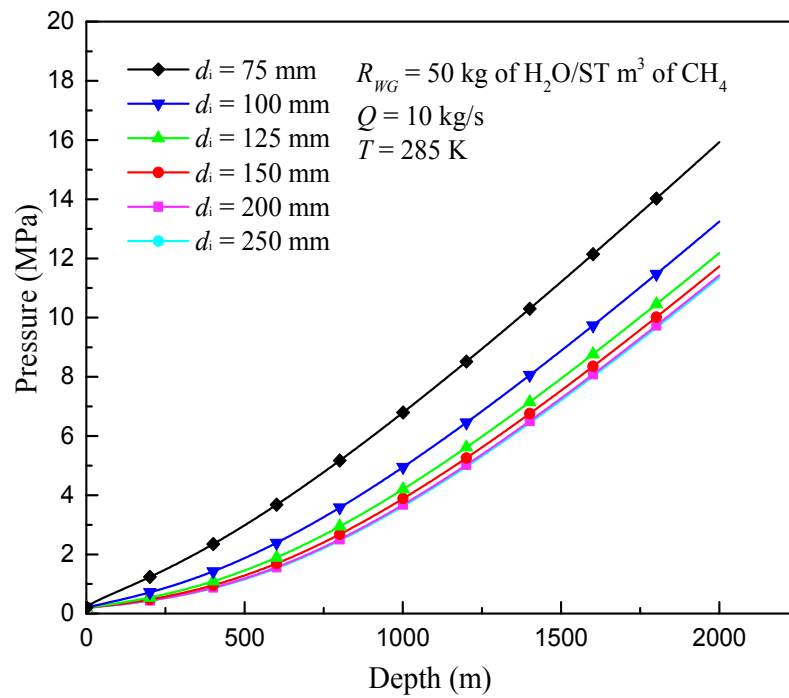**Figure 10.** Velocity distributions along the vertical pipe under different R_{WG} (kg H_2O/Nm^3 CH_4).
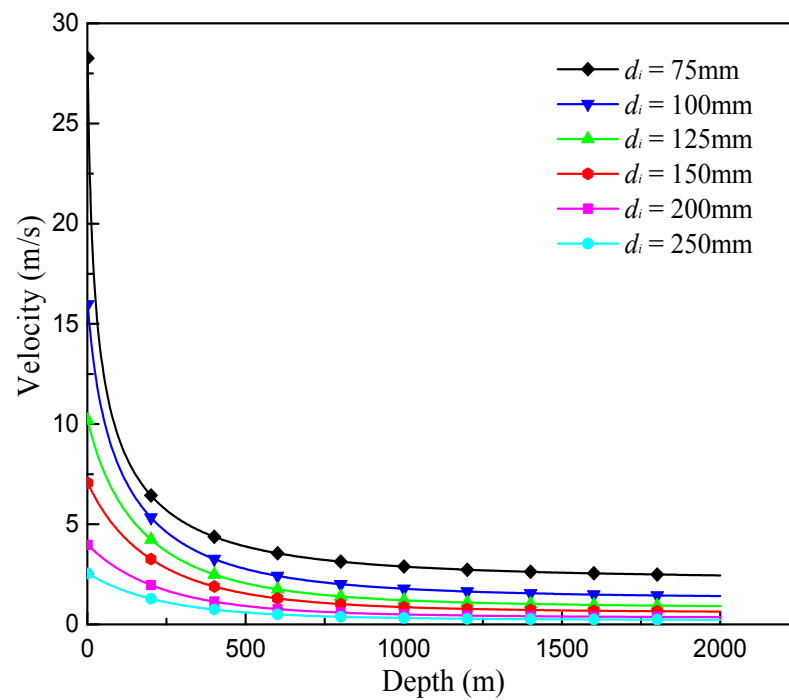
3.3.2. Effects of Inner Diameter of the Vertical Pipe

Figures 11 and 12 show the effects of a range of inner diameter d_i from 75 to 250 mm on the pressure and velocity of fluid, respectively. The R_{WG} in this case is 50 kg H_2O/Nm^3 CH_4. The distribution of pressure and velocity increase with the decrease of inner diameter, the smaller inner diameter shows more significant influence on pressure and velocity. For d_i = 75 mm, the bottomhole pressure reaches 16 MPa, which is beyond the P_{wf} calculated in 200 mm pipe. The outlet flow velocity at the ocean surface reaches 28 m/s. Such a high flow velocity is very detrimental for the flow control of gas production and would increase the energy consumption of the fluids transportation greatly.
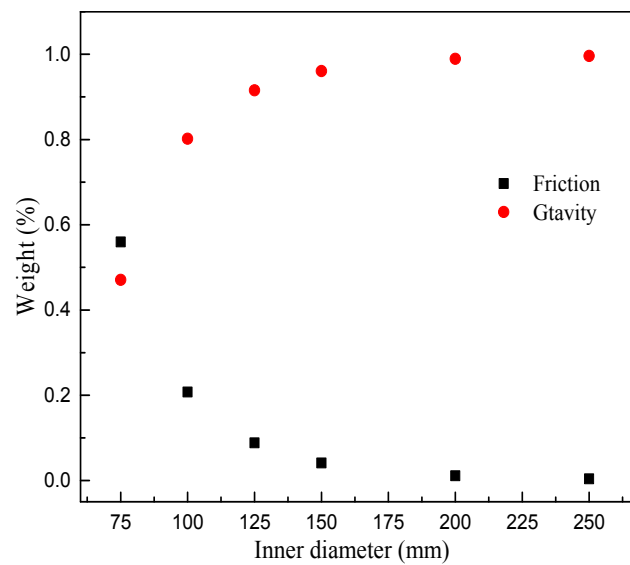
Figure 13 shows the weight of the friction and gravity pressure drop under the conditions of different inner diameters. The friction pressure drop increases rapidly when d_i decreases to less than 125 mm and correspondingly, the weight of gravity pressure drop decreases. For d_i = 75 mm, the friction pressure drop accounts for over 56% of the total pressure drop because the large friction force between the mixed fluid and the inner wall of the vertical pipe. As d_i exceeds 100 mm, the gravity pressure drop becomes dominant, especially for d_i = 200 mm and d_i = 250 mm. It is suggested that the friction pressure drop is not more than 5% of total pressure drop in oil production [40]. So, a large diameter pipe is suggested in NGH production.

Figure 11. Pressure distributions along the vertical pipe with different pipe inner diameters.
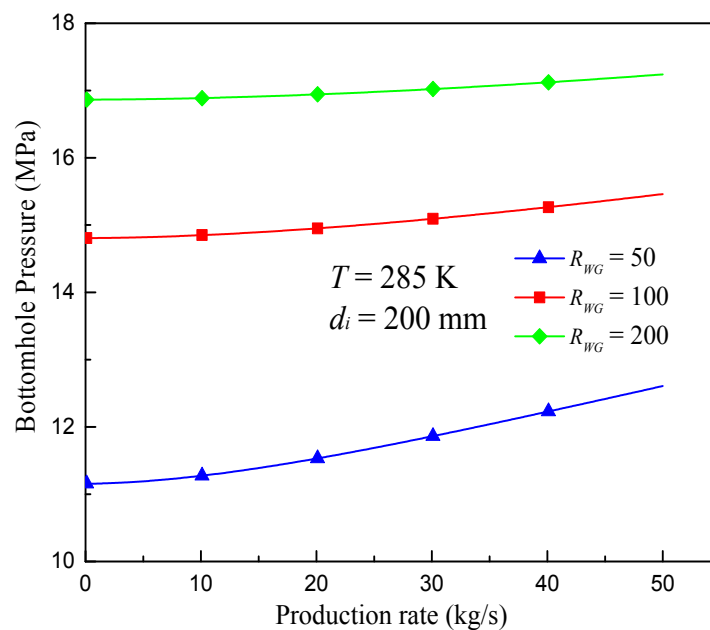

Figure 12. Velocity distributions along the vertical pipe with different pipe inner diameters.

Figure 13. Proportion of pressure loss with different pipe inner diameters.

3.3.3. Effects of Two Phase Flow Rate

Flow rate of methane-water mixture q is a key issue for depressurization method, which directly affects the NGH dissociation and seepage in deposits. The effect of the flow rate of methane-water mixture on the P_{wf} with different R_{WG} (50, 100, 200 kg H_2O/Nm^3 CH_4) are shown in Figure 14. As q increases from 0 to 50 kg/s, the P_{wf} increase slightly in each R_{WG}. This indicates that the flow rate of methane-water mixture q has a weaker effect on the P_{wf} compared to the inlet water-gas ratio R_{WG}. The decrease of R_{WG} slightly enhances the effect of q on P_{wf}. In essence, the R_{WG} is strong related to the density of fluid, which determines the pressure gradient, while the increasing q only weakly affects the friction and acceleration pressure drop.

Figure 14. Effect of the flow rate of methane-water mixture on the bottomhole pressure with different R_{WG} (kg H_2O/Nm^3 CH_4).

4. Conclusions

A gas-lifting method was firstly proposed to transport methane-water mixture from natural gas hydrates deposits in this work to make full use of the lifting ability of the produced methane. We established a two-phase flow model and validated it by comparing pressure prediction with traditional models in oil and gas wells. Compared to the traditional models, the new model needs not empirical correlations and is more suitable for NGH production.

The calculation results indicate that the gas-lifting method has great advantage in avoiding the formation of secondary hydrates in the vertical pipe. The gas-lifting process in the vertical pipe is spontaneous in UBGH2-6 site and SH7 site during the initial 4000 and 1000 days, respectively and thus the energy consumption for transportation of methane-gas mixture is avoided. Self-eruption production of gas hydrates could be a potential mining method if sufficient heat supply for gas hydrate dissociation is sufficient.

Water-gas ratio has more significant effect on the bottomhole pressure as compared to flow rate. The bottomhole pressure decreases rapidly when water-gas ratio is less than 100 kg H_2O/Nm^3 CH_4. Reducing water production can significantly improve the gas-lifting performance of methane-water mixture in vertical pipe. Impermeable boundaries and higher production pressure employed are two important factors which could benefit the spontaneous gas lifting process and the NGH self-eruption production.

Author Contributions: The research study was carried out successfully with contribution from all authors. The main research idea was contributed by Zhaoyang Chen, Xiaosen Li and Jinming Zhang. Jinming Zhang contributed on the simulation works, manuscript preparation and research idea. Yu Zhang, Gang Li and Kefeng Yan assisted with finalizing the research work and manuscript, Tao Lv provided several suggestions from the oil and gas industrial perspectives. All authors revised and approved the publication of the paper.

Conflicts of Interest: The authors declare no conflict of interest.

Nomenclature

C	correction factor
C_g	specific heat of gas (KJ/kg)
C_l	specific heat of water (KJ/kg)
d_i	pipe inner diameter (m)
g	gravitational acceleration (m/s^2)
K	intrinsic permeability (m^2)
M_{CH_4}	molar mass of methane (kg/mol)
m_g	dissociated gas mass of per unit mass of hydrate (kg)
m_l	dissociated water mass of per unit mass of hydrate (kg)
n	correction factor
N_h	quantity of heat used for hydrate dissociation (mol)
P	methane-water mixture pressure (Pa)
P_c	critical pressure (Pa)
P_{out}	outlet pressure at ocean surface (Pa)
P_r	constant production pressure (Pa)
P_{wf}	bottomhole pressure (Pa)
q	flow rate methane-water mixture (kg/s)
Q_h	molar quantity of hydrate dissociation (KJ)
Q_R	heat release of the system during the hydrate dissociation process (KJ)

Q_{sur}	heat transfer from surrounding water to the per unit mass of hydrate (KJ/kg)
R	gas constant (J/mol·K)
Re	methane-water mixture Reynolds number
r_w	radius of hydrate-bearing-layer (m)
R_{WG}	water-gas ratio (kg H_2O/Nm^3 CH_4)
S	methane solubility in seawater (kg/kg)
S_0	methane solubility in seawater under bottomhole condition (kg/kg)
T	methane-water mixture temperature (K)
T_c	critical temperature (K)
T_r	reduced temperature (K)
u	methane-water mixture velocity (m/s)
v	gas specific volume (m^3/kg)
W	work exchange between surroundings and the system (KJ)
z	vertical pipe depth (m)
$-(\partial P_f/\partial z)$	frictional pressure gradient (Pa/m)
Z	gas compression factor
ρ	mixture density (kg/m^3)
ρ^g	gas density (kg/m^3)
ρ^l	seawater density (kg/m^3)
μ	methane-water mixture viscosity (Pa·s)
δ	gas mass fraction in mixture (kg/kg)
δ_0	gas mass fraction in mixture under inlet condition (kg/kg)
ΔN_h	dissociation heat of hydrate (KJ/mol)
ΔE_k	change of kinetic energy from the reservoir condition to the surface condition (KJ)
ΔE_p	change of potential energy from the reservoir condition to the surface condition (KJ)

References

1. Sloan, E.D.; Koh, C.A. *Clathrate Hydrates of Natural Gases*, 3rd ed.; CRC Press: Boca Raton, FL, USA, 2007; p. 721.
2. Makogon, Y.F. *Hydrates of Natural Gas*; In PennWell: Tulsa, OK, USA, 1981.
3. Boswell, R.; Collett, T.S. Current perspectives on gas hydrate resources. *Energy Environ. Sci.* **2011**, *4*, 1206–1215. [CrossRef]
4. Milkov, A.V. *How and Why the Global Estimates of Hydrate-Bound Gas in Marine Sediments Decreased over the Last Thirty Years and What this Means for Resources and Global Change Evaluations*; American Geophysical Union: Washington, DC, USA, 2003.
5. Makogon, Y.F.; Holditch, S.A.; Makogon, T.Y. Natural gas-hydrates—A potential energy source for the 21st Century. *J. Petrol. Sci. Eng.* **2007**, *56*, 14–31. [CrossRef]
6. Japan Oil, Gas and Metals National Corporation (GOGMEC). Gas Produced from Methane Mydrate (Provisional). 2013. Available online: http://www.jogmec.go.jp/english/news/release/news_01_000006.html (accessed on 19 March 2013).
7. Natural Gas World. China Successfully Completes First Gas Hydrate Trial. 2017. Available online: http://www.jwnenergy.com/article/2017/8/china-successfully-completes-first-gas-hydrate-trial (accessed on 1 August 2017).
8. Yin, Z.Y.; Chong, Z.R.; Tan, H.K.; Linga, P. Review of gas hydrate dissociation kinetic models for energy recovery. *J. Nat. Gas. Sci. Eng.* **2016**, *35*, 1362–1387. [CrossRef]
9. Li, G.; Moridis, G.J.; Zhang, K.N.; Li, X.S. Evaluation of gas production potential from marine gas hydrate deposits in Shenhu Area of South China Sea. *Energy Fuels* **2010**, *24*, 6018–6033. [CrossRef]
10. Moridis, G.J.; Reagan, M.T.; Boyle, K.L.; Zhang, K.N. Evaluation of the gas production potential of some particularly challenging types of oceanic hydrate deposits. *Transp. Porous Med.* **2011**, *90*, 269–299. [CrossRef]
11. Brill, J.P. Multiphase Flow in Wells. *J. Petrol. Technol.* **1987**, *39*, 15–21. [CrossRef]
12. Moridis, G.J.; Reagan, M.T. Strategies for gas production from oceanic class 3 hydrate accumulations. In Proceedings of the 2007 Offshore Technology Conference, Houston, TX, USA, 30 April–3 May 2007.

13. Moridis, G.J.; Collett, T.S.; Boswell, R.; Kurihara, M.; Reagan, M.T.; Koh, C.; Sloan, E.D. Toward Production From Gas Hydrates: Current Status, Assessment of resources and simulation-based evaluation of technology and potential. *SPE Reserv. Eval. Eng.* **2009**, *12*, 745–771. [CrossRef]

14. Moridis, G.J.; Reagan, M.I.; Kim, S.J.; Seol, Y.; Zhang, K. Evaluation of the gas production potential of marine hydrate deposits in the Ulleung Basin of the Korean East Sea. *SPE J.* **2009**, *14*, 759–781. [CrossRef]

15. Konno, Y.; Fujii, T.; Sato, A.; Akamine, K.; Naiki, M.; Masuda, Y.; Yamamoto, K.; Nagao, J. Key findings of the world's first offshore methane hydrate production test off the coast of Japan: Toward future commercial production. *Energy Fuels* **2017**, *31*, 2607–2616. [CrossRef]

16. Heeschen, K.U.; Abendroth, S.; Priegnitz, M.; Spangenberg, E.; Thaler, J.; Schicks, J.M. Gas production from methane hydrate: A laboratory simulation of the multistage depressurization test in Mallik, Northwest Territories, Canada. *Energy Fuels* **2016**, *30*, 6210–6219. [CrossRef]

17. Li, G.; Li, B.; Li, X.S.; Zhang, Y.; Wang, Y. Experimental and numerical studies on gas production from methane hydrate in porous media by depressurization in pilot-scale hydrate simulator. *Energy Fuels* **2012**, *26*, 6300–6310. [CrossRef]

18. Moridis, G.J.; Kim, J.; Reagan, M.T.; Kim, S.J. Feasibility of gas production from a gas hydrate accumulation at the UBGH2-6 site of the Ulleung basin in the Korean East Sea. *J. Petrol. Sci. Eng.* **2013**, *108*, 180–210. [CrossRef]

19. Zhang, Y.X. Methane escape from gas hydrate systems in marine environment and methane-driven oceanic eruptions. *Geophys. Res. Lett.* **2003**, *30*, 325–348. [CrossRef]

20. Giot, M. Three phase flow. In *Handbook of Multiphase Systems*; McGraw-Hill Book Co.: New York, NY, USA, 1982; Volume 7.

21. Hasan, A.R.; Kabir, C.S.; Sayarpour, M. Simplified two-phase flow modeling in wellbores. *J. Petrol. Sci. Eng.* **2010**, *72*, 42–49. [CrossRef]

22. Wilson, L.; Sparks, R.S.J.; Walker, G.P.L. Explosive volcanic-eruptions. 4. The control of magma properties and conduit geometry on eruption column behavior. *Geophys. J. R. Astr. Soc.* **1980**, *63*, 117–148. [CrossRef]

23. Soave, G. Equilibrium constants from a modified Redlich-Kwong equation of state. *Chem. Eng. Sci.* **1972**, *27*, 1197–1203. [CrossRef]

24. Duan, Z.H.; Moller, N.; Greenberg, J.; Weare, J.H. The prediction of methane solubility in natural-waters to high ionic-strength from 0 to 250 °C and from 0 to 1600 bar. *Geochim. Cosmochim. Acta* **1992**, *56*, 1451–1460. [CrossRef]

25. Feng, J.C.; Wang, Y.; Li, X.S.; Chen, Z.Y.; Li, G.; Zhang, Y. Investigation into optimization condition of thermal stimulation for hydrate dissociation in the sandy reservoir. *Appl. Energy* **2015**, *154*, 995–1003. [CrossRef]

26. Zhang, Y.X. Energetics of gas-driven limnic and volcanic eruptions. *J. Volcanol. Geotherm. Res.* **2000**, *97*, 215–231. [CrossRef]

27. Hagedorn, A.R.; Brown, K.E. Experimental study of pressure gradients occurring during continuous two-phase flow in small-diameter vertical conduits. *J. Petrol. Technol.* **1965**, *17*, 475–484. [CrossRef]

28. Orkiszewski, J. Predicting two-phase pressure drops in vertical pipe. *J. Petrol. Technol.* **1967**, *19*, 829–838. [CrossRef]

29. Aziz, K.; Fogarasi, M.; Govier, G.W. Pressure-drop in wellsproducing oil and gas. *J. Can. Petrol. Technol.* **1972**, *11*, 38–47. [CrossRef]

30. Ansari, A.M.; Sylvester, N.D.; Sarica, C.; Shoham, O.; Brill, J.P. A comprehensive mechanistic model for upward two-phase flow in wellbores. *SPE Prod. Facil.* **1994**, *9*, 143–152. [CrossRef]

31. Beggs, H.D.; Brill, J.P. Study of two-Phase Flow in Inclined Pipes. *J. Petrol. Technol.* **1973**, *25*, 607–617. [CrossRef]

32. Mukherjee, H.; Brill, J.P. Pressure-drop correlations for inclined two-phase flow. *J. Energy Resour. Technol.* **1985**, *107*, 549–554. [CrossRef]

33. Hasan, A.R.; Kabir, C.S.; Sarica, C. *Fluid Flow and Heat Transfer in Wellbores*; Society of Petroleum Engineers: Richardson, TX, USA, 2002.

34. Hibiki, T.; Ishii, M. One-dimensional drift-flux model for two-phase flow in a large diameter pipe. *Int. J. Heat Mass Transf.* **2003**, *46*, 1773–1790. [CrossRef]

35. Shi, H.; Holmes, J.A.; Durlofsky, L.J.; Aziz, K.; Diaz, L.R.; Alkaya, B.; Oddie, G. Drift-flux modeling of two-phase flow in wellbores. *SPE J.* **2005**, *10*, 24–33. [CrossRef]

36. Bhagwat, S.M.; Ghajar, A.J. A flow pattern independent drift flux model based void fraction correlation for a wide range of gas-liquid two phase flow. *Int. J. Multiph. Flow* **2014**, *59*, 186–205. [CrossRef]

37. Wang, Y.; Feng, J.C.; Li, X.S.; Zhang, Y.; Li, G. Evaluation of gas production from marine hydrate deposits at the GMGS2-Site 8, Pearl River Mouth Basin, South China Sea. *Energies* **2016**, *9*, 222. [CrossRef]
38. Zhang, Y.X. Dynamics of CO2-driven lake eruptions. *Nature* **1996**, *379*, 57–59. [CrossRef]
39. Kennett, J.P.; Cannariato, K.G.; Hendy, I.L.; Behl, R.J. Carbon isotopic evidence for methane hydrate instability during quaternary interstadials. *Science* **2000**, *288*, 128–133. [CrossRef] [PubMed]
40. Gregory, G.A.; Fogarasi, M.; Aziz, K. Analysis of vertical two-phase flow calculations-crude oil-gas flow in well tubing. *J. Can. Petrol. Technol.* **1980**, *19*, 86–92. [CrossRef]